constant of approximately $10^7$ L mol$^{-1}$ s$^{-1}$ for $SO_2/SO_2^-$. If the collision diameter is lowered to 2.5 Å,[30a] the self-exchange rate constant obtained is $\sim 10^4$ L mol$^{-1}$ s$^{-1}$. The choice of $r$ at the short contact distances appropriate to these reactions is obviously critical and somewhat arbitrary.[30b]

The choice of a $k_{22}$ value is also troublesome. Almost certainly, each viologen will have a unique value of $k_{22}$ and this value will *not* be constant for the viologens used. In fact, analysis by Tsukahara and Wilkins[4] indicates that the self-exchange rate constant for the BDQ couple is ~20 times less than that for the PDQ couple. However, there does appear to be a reliable estimate for $MV^{2+}/MV^+$ of $8 \times 10^5$ L mol$^{-1}$ s$^{-1}$.[29] For the reduction of $MV^{2+}$ by $Cr^{2+}$, $V^{2+}$, $*[Ru(bpy)_3]^{2+}$, and $[Ru(bpy)_3]^{2+}$, the value of $8 \times 10^5$ M$^{-1}$ s$^{-1}$ gives good agreement between calculated and observed reductant self-exchange rate constants except for the case of $[Ru(bpy)_3]^{2+}$. Use of this exchange value, however, gives $SO_2/SO_2^-$ self-exchange constants at or above the diffusion-controlled limit. Thus, the values obtained must be viewed with caution. In light of the known charge-transfer interactions between $SO_2^-$ and aromatic organic molecules,[26b] it may be that the reactions considered are not simple outer-sphere reactions.

The remaining estimate of the $SO_2/SO_2^-$ rate constant[11] of approximately $10^7$ L mol$^{-1}$ s$^{-1}$, from comparison of the reactions of $SO_2^-$ and $O_2^-$, suffers from the lack of a reliable $k_{11}$ value for $O_2/O_2^-$. Estimates for $k_{11}$ obtained from cross-reactions are not constant but in fact vary from $10^{-6}$ to $10^5$ L mol$^{-1}$ s$^{-1}$.[32]

Finally, by use of the Marcus theory, the rate constant for the self-exchange reaction can be predicted from structural data:[10]

$$k_{ex} = Z \exp[-(w_r + \Delta G^*_{in} + \Delta G^*_{out})/RT]$$

From the values calculated by Stanbury and Lednicky[9] for the activation energies to rearrange the inner, $\Delta G^*_{in}$, and outer, $\Delta G^*_{out}$, "coordination" spheres and work terms, $w_r$, from eq 8, a value of $1.1 \times 10^3$ M$^{-1}$ s$^{-1}$ can be obtained. The excellent agreement between this calculated value and the value derived from the cross-reactions in this study, $\sim 10^3$ M$^{-1}$ s$^{-1}$, clearly demonstrates the applicability of the Marcus theory to dithionite reductions.

In conclusion, this study has shown that $SO_2^-$ is an effective reducing agent for a wide variety of complexes and reacts by a simple outer-sphere pathway. A reasonable value for the $SO_2/SO_2^-$ exchange rate constant is obtained from the Marcus reactive collision model when applied to these systems. It is also necessary to consider work terms in the calculations when the collision diameter is small. Although most reactions involving dithionite proceed via the $SO_2^-$ radical, under appropriate conditions $S_2O_4^{2-}$ can also be an effective reducing agent. Further work is necessary to characterize the reactivity of undissociated dithionite.

**Acknowledgment.** We thank Dr. Y. Kotake and Prof. E. Janzen for the ESR measurements and the Natural Sciences and Engineering Research Council for support of this work.

**Registry No.** *trans*-$[Co(cyclam)(NH_3)_2]^{3+}$, 53176-75-3; *trans*-$[Co(cyclam)Cl_2]^+$, 19973-61-6; $[Co(sep)]^{3+}$, 72496-77-6; $[Co(diamsar)]^{3+}$, 85663-96-3; $[Co(bpy)_3]^{3+}$, 19052-39-2; $[Co(NH_3)_6]^{3+}$, 14695-95-5; $[Co(NH_3)_5(4\text{-}NO_2\text{-}imid)]^{2+}$, 110682-59-2; $[Co(NH_3)_5imid]^{3+}$, 38716-02-8; $[Co(NH_3)_5imid]^{2+}$, 61159-81-7; $[Co(NH_3)_5pyz]^{3+}$, 59389-55-8; $[Co(NH_3)_5(4,4'\text{-}bpy)]^{3+}$, 53879-90-6; $[Co(NH_3)_5py]^{3+}$, 31011-67-3; $[Ru(NH_3)_5pyz]^{3+}$, 38139-16-1; $[Fe(CN)_5py]^{2-}$, 61332-63-6; $[Fe(CN)_5(4,4'\text{-}bpy)]^{2-}$, 84823-86-9; $[Fe(CN)_5imid]^{2-}$, 61332-60-3; $[Fe(CN)_5pyz]^{2-}$, 61332-65-8; $[Ru(NH_3)_5imid]^{3+}$, 80593-52-8; $[Fe(CN)_5bpy]^{2-}$, 73295-95-1; $SO_2^-$, 12143-17-8; $S_2O_4^{2-}$, 14844-07-6.

**Supplementary Material Available:** A table of kinetic data for reduction of Co(III), Fe(III), and Ru(III) by dithionite (4 pages). Ordering information is given on any current masthead page.

(30) (a) An extreme view with respect to ref 26a and may imply charge-transfer complex formation. (b) Rosseinsky, D. *Comments Inorg. Chem.* **1984**, *3*, 153.
(31) Balahura, R. J.; Ferguson, G., Ruhl, B., Wilkins, R. G. *Inorg. Chem.* **1983**, *22*, 3990.
(32) Espenson, J.; Bakac, A.; McDowell, M. S. *Inorg. Chem.* **1984**, *23*, 2232.

Contribution from the Department of Chemistry, State University of New York at Stony Brook, Stony Brook, New York 11794-3400

# Synthetic and Structural Studies of Phosphine and Phosphite Derivatives of the $[FeCo_3(CO)_{12}]^-$ Anion and Their $[Ph_3PAu]^+$ Adducts

Arthur A. Low and Joseph W. Lauher*

*Received February 25, 1987*

Synthetic and structural studies of phosphine- and phosphite-substituted derivatives of $[FeCo_3(CO)_{12}]^-$ and $[Ph_3PAuFeCo_3(CO)_{12}]$ are reported. The anion reacts with phosphine or phosphites to yield monosubstituted derivatives of the formula $[FeCo_3(CO)_{11}L]^-$. When L = $P(OMe)_3$ or $PMe_2Ph$, $[Ph_3PAuNO_3]$ reacts with $[FeCo_3(CO)_{11}L]^-$ to give substituted gold derivatives. For L = $P(OMe)_3$, the isolated product is the disubstituted gold compound $[Ph_3PAuFeCo_3(CO)_{10}\{P(OMe)_3\}_2]$. When L = $PPh_3$, no reaction is observed with $[Ph_3PAuNO_3]$. Crystal structures of the compounds $[Et_4N][FeCo_3(CO)_{11}PPh_3]$, $[Co(CO)\{P(OMe)_3\}_4]$-$[FeCo_3(CO)_{11}P(OMe)_3]$, $[Ph_3PAuFeCo_3(CO)_{11}PMe_2Ph]$, and $[Ph_3PAuFeCo_3(CO)_{10}\{P(OMe)_3\}_2]$ are reported. Significant angular distortions are found in the packing of the carbonyl ligands. In the substituted gold derivatives, the $Ph_3PAu$ moiety is significantly distorted from the symmetrical position observed in $[Ph_3PAuFeCo_3(CO)_{12}]$.

In a preliminary report several years ago we published a structural study of the trigonal-bipyramidal cluster, $[Ph_3PAuFeCo_3(CO)_{12}]$, the first example of a cluster with an Au atom triply bridging three transition-metal atoms.[1] In that report, we noted a close structural relationship between certain hydrido-metal complexes and the corresponding $[Ph_3PAu]^+$ adducts. Our proposed gold-hydride analogy has been further explored by others, and many new gold cation adducts of transition-metal cluster anions have been reported.[2] Most gold derivatives have indeed proved to be structural analogues of the corresponding hydride complexes, but many have not.

The structural relationships between gold phosphine and hydride derivatives have thus proved to be subtle and are not yet defined. Few direct comparisons of the reaction chemistry of hydrides and the corresponding gold complexes have been reported.

(1) Lauher, J. W.; Wald, K. *J. Am. Chem. Soc.* **1981**, *103*, 7648.
(2) Hall, K. P.; Mingos, D. M. P. *Prog. Inorg. Chem.* **1984**, *32*, 237-326 and references therein.

0020-1669/87/1326-3863$01.50/0 

**Table I.** Crystal Data Parameters[a]

| | $[Et_4N][1]$ | $[Co(CO)\{P(OMe)_3\}_4][2]$ | **4** | **3** |
|---|---|---|---|---|
| formula | $C_{37}H_{35}FeCo_3PO_{11}N$ | $C_{27}H_{45}FeCo_4P_5O_{27}$ | $C_{44}H_{33}AuCo_3FeP_3O_{16}$ | $C_{34}H_{31}AuFeCo_3P_2O_{11}$ |
| fw | 933.30 | 1248.08 | 1340.27 | 1107.17 |
| $a$, Å | 12.737 (1) | 10.605 (5) | 21.566 (5) | 22.863 (14) |
| $b$, Å | 14.038 (4) | 32.842 (7) | 13.356 (3) | 13.232 (4) |
| $c$, Å | 11.466 (2) | 14.331 (6) | 15.141 (2) | 28.598 (6) |
| $\alpha$, deg | 94.87 (3) | | | |
| $\beta$, deg | 97.98 (1) | 93.08 (3) | | 95.28 (9) |
| $\gamma$, deg | 79.77 (2) | | | |
| $V$, Å$^3$ | 1194 (11) | 4991 (5) | 4361 (3) | 8615 (8) |
| cryst syst | triclinic | monoclinic | orthorhombic | monoclinic |
| space group | $P\bar{1}$ | $P2_1/c$ | $Pna2_1$ | $C2/c$ |
| $Z$ | 2 | 4 | 4 | 8 |
| $d_{calcd}$, g cm$^{-3}$ | 1.554 | 1.661 | 1.858 | 1.707 |
| abs coeff ($\mu$), cm$^{-1}$ | 17.396 | 18.872 | 51.334 | 51.438 |
| cryst dimens, mm | 1.33 × 0.45 × 0.10 | 0.075 × 0.175 × 0.45 | 0.20 × 0.40 × 0.30 | 0.500 × 0.475 × 0.225 |
| $2\theta$ range, deg | 0–52 | 0–45 | 0–50 | 0–48 |
| $F$(000) | 948 | 2528 | 2384 | 4312 |
| no. of reflcns collcd | 8666 | 5181 | 5376 | 5721 |
| cutoff | $I \geq 3\sigma(I)$ | $I \geq 3\sigma(I)$ | $I \geq 3\sigma(I)$ | $I \geq 3\sigma(I)$ |
| no. of obsd reflcns | 6021 | 2213 | 2822 | 1913 |
| no. of variables | 478 | 577 | 522 | 256 |
| cryst faces | irregular | (101), (010), (001) ($\bar{1}$00), (0$\bar{1}$0), (00$\bar{1}$) | (100), (010), (001) ($\bar{1}$00), (0$\bar{1}$0), (00$\bar{1}$) | (100), (11$\bar{2}$), ($\bar{1}$,22) ($\bar{1}$00), ($\bar{1}\bar{1}$2), (2$\bar{3}\bar{3}$) |
| $h,k,l$ range | ±13,±14,+12 | ±10,+31,+13 | +24,+15,+18 | +24,+12,±18 |
| trans fact (min, max) | | 13.63, 87.03 | 15.65, 53.13 | 11.09, 38.81 |
| $R$ | 0.046 | 0.048 | 0.041 | 0.089 |
| $R_w$ | 0.0586 | 0.069 | 0.049 | 0.101 |

[a] All data were collected on a Enraf-Nonius CAD-4A diffractometer using graphite-monochromated Mo K$\alpha$ (0.71073 Å) radiation.

We have continued our own studies in this area and would now like to report the results of our subsequent synthetic and structural studies of the $[FeCo_3(CO)_{12}]^-$ anion and its $[Ph_3PAu]^+$ adduct. We have used phosphine and phosphite substitution as our probe of the chemical and structural properties of these compounds. As the reader will soon discover, our studies are still not complete due to the complex equilibrium involved, but considerable progress has been made.

## Experimental Section

All reactions were carried out under a dry nitrogen atmosphere with stainless steel cannulas used for transferring solutions (unless otherwise noted). Column chromatography was performed in the air. Reaction solvents were dried over appropriate drying agents and distilled before use. The reagents $P(OMe)_3$, $PMe_2Ph$ (Strem), and $PPh_3$ (Alfa) were used as received. $[Ph_3PAuNO_3]$ was made according to literature procedures.[3] $[Et_4N][FeCo_3(CO)_{12}]$ was synthesized by the method of Chini,[4] with some modifications.[5] $[Et_4N][FeCo_3(CO)_{11}PPh_3]$ was prepared according to the method of Mays.[6]

IR spectra were recorded on a Perkin-Elmer 467 spectrometer using KCl solution cells. Peaks are reported in cm$^{-1}$ and were calibrated against polystyrene. $^1$H FT-NMR were recorded on a Varian NT-100 80 MHz spectrometer. Resonances are reported as shifts in ppm downfield from tetramethylsilane.

**$[Ph_3PAuFeCo_3(CO)_{10}\{P(OMe)_3\}_2]$. Step 1** ($P(OMe)_3$ substitution of $[FeCo_3(CO)_{12}]^-$ anion). To a solution of 1 g of $[Et_4N][FeCo_3(CO)_{12}]$ (1.43 mmol) in 20 mL of acetone was added 0.4 mL of $P(OMe)_3$ (0.42 g, 3.4 mmol) via syringe. The solution was refluxed for 4 h, during which time the color of the solution changed from red-brown to purple. After removal of the solvent under vacuum, the oily residue was dissolved in 1 mL of $CHCl_3$ and chromatographed on a neutral alumina column with 9:1 $CHCl_3$–$CH_2Cl_2$ mixtures. The first band eluted was yellow-brown in color and was identified as $Fe(CO)_{5-n}[P(OMe)_3]_n$ ($n$ = 1–3) mixtures by an examination of the carbonyl region of the infrared spectrum. As the percentage of $CH_2Cl_2$ was increased, a purple band was eluted. This fraction contained the $[FeCo_3(CO)_{11}P(OMe)_3]^-$ anion, as identified by an examination of the carbonyl region of its infrared spectrum. The identity of the accompanying cation was not clear as explained in the text. After removal of the solvent in vacuum, 0.96 g of a purple oil remained. IR ($CH_2Cl_2$, cm$^{-1}$): 2040 w, 1995 s, 1970 sh, 1905 m, 1840 w, 1782 m.

**Step 2.** The oil from step 1 was dissolved in 10 mL of $CH_2Cl_2$. To this solution was added a solution of 0.75 g of $[Ph_3PAuNO_3]$ (1.44 mmol) in 10 mL of $CH_2Cl_2$. The color of the solution immediately changed from purple to a deep blue. After 5 min, the solvent was removed in vacuum. The residue left over was extracted with 10-mL portions of 9:1 benzene–chloroform until the extracts were colorless. The solvent was removed from the extracts and the residue was recrystallized from toluene–hexanes. Yield: 0.47 g (27% based on $[Et_4N][FeCo_3(CO)_{12}]$). IR ($CCl_4$, cm$^{-1}$): 2060 m, 2015 s, 1994 s, 1986 s, 1910 sh, 1862 m, 1842 m. NMR (benzene-$d_6$): $\delta$ 6.99 (m, ≈5 H), 3.21 (d, $J$ = 11.21 Hz, 6 H). Anal. Calcd for $C_{34}H_{33}P_3AuFeCo_3O_{16}$: C, 33.47; H, 2.73. Found: C, 34.90; H, 2.74.

**$[Ph_3PAuFeCo_3(CO)_{11}PMe_2Ph]$. Step 1** ($PMe_2Ph$ substitution of $[FeCo_3(CO)_{12}]^-$ anion). To a solution of 1.0 g of $[Et_4N][FeCo_3(CO)_{12}]$ (1.43 mmol) in 20 mL of acetone was added 0.4 mL of $PMe_2Ph$ (2.81 mmol) via syringe. The solution was refluxed for 12 h. After removal of the solvent in vacuum, further purification procedures followed the same procedure described above. IR ($CH_2Cl_2$, cm$^{-1}$): 2035 w, 2000 w, 1985 s, 1960 sh, 1910 m, 1785 m br.

**Step 2.** The synthesis of purification of $[Ph_3PAuFeCo_3(CO)_{11}PMe_2Ph]$ followed the same procedure as described for the $P(OMe)_3$-substituted product. IR ($CCl_4$, cm$^{-1}$): 2060 m, 2015 s, 1996 s 1986 m, 1975 sh, 1854 m, 1830 m. $^1$H NMR (benzene-$d_6$): $\delta$ 7900 (m, ≈10 H), 1.39 (d, $J$ = 8.8 Hz, 4 H).

## Crystallographic Analyses

The general method used for the single-crystal X-ray structure determination is described below. The specifics for each structure follow. Each crystal, except for compound **4**, was glued onto a glass fiber and mounted on an Enraf-Nonius CAD4 diffractometer controlled by a PDP 11/45 computer. Compound **4** was placed inside a thin-walled glass capillary containing mineral oil.

Cell constants and their corresponding standard deviations were derived by a least-squares refinement of the settings of 25 reflections that had been located and centered by the diffractometer. Once a consistent unit cell had been determined, higher $2\theta$ angle data (20–25°) was quickly collected and the centering procedures were repeated in order to obtain a better quality unit cell. The most probable space group was then determined from the systematic absences. From the 25 higher angle peaks, three were chosen as intensity controls and two were chosen as orientation controls to be checked periodically throughout the data collection. Data were collected at 25 °C by using the $\omega/2\theta$ method. Crystallographic data for all compounds are listed in Table I. Tables of positional and thermal parameters of the core atoms are listed in Table II. Average bond distances and angles are listed in Tables III and IV.

(3) Maltesta, L.; Naldini, L.; Simonetta, A.; Cariati, F. *Coord. Chem. Rev.* **1966**, *1*, 255.
(4) Chini, P.; Colli, L.; Peraldo, M. *Gazz. Chim. Ital.* **1960**, *90*, 1005.
(5) Sherlock, S.; Low. A. .; Lauher, J. W., to be submitted for publication in *Inorg. Chem.*
(6) Cooke, C. G.; Mays, M. J. *J. Organomet. Chem.* **1974**, *74*, 449.
(7) Molecular graphics package written by J. Lauher.

**Table II.** Selected Positional and Thermal Parameters and Estimated Standard Deviations[a]

| atom | x | y | z | B,[b] Å² |
|---|---|---|---|---|
| | | [Et₄N][1] | | |
| Co1 | 0.21219 (5) | 0.73589 (4) | 0.21933 (5) | 2.17 (2) |
| Co2 | 0.34370 (5) | 0.79788 (5) | 0.37643 (6) | 2.76 (2) |
| Co3 | 0.34901 (5) | 0.61811 (5) | 0.33635 (6) | 2.58 (2) |
| Fe1 | 0.41166 (6) | 0.71595 (6) | 0.18954 (7) | 3.21 (3) |
| P | 0.0524 (1) | 0.75178 (9) | 0.2861 (1) | 2.19 (4) |
| | | $[Co(CO)\{P(OMe)_3\}_4]$[2] | | |
| Co1 | −0.0763 (2) | 0.39889 (8) | 0.2915 (2) | 2.80 (9) |
| Co2 | 0.1074 (2) | 0.44490 (8) | 0.3003 (2) | 2.88 (10) |
| Co3 | 0.1061 (2) | 0.38991 (8) | 0.1847 (2) | 2.83 (9) |
| Co4 | 0.5110 (2) | 0.15702 (7) | 0.3054 (2) | 2.27 (9) |
| Fe | 0.1314 (3) | 0.37214 (9) | 0.3554 (2) | 3.1 (1) |
| P1 | −0.2216 (5) | 0.4288 (2) | 0.2121 (3) | 2.9 (2) |
| P2 | 0.5799 (5) | 0.1012 (2) | 0.2424 (3) | 2.7 (2) |
| P3 | 0.3369 (5) | 0.1260 (2) | 0.3371 (3) | 2.9 (2) |
| P4 | 0.4421 (5) | 0.1971 (2) | 0.1957 (3) | 3.1 (2) |
| P5 | 0.6974 (5) | 0.1829 (2) | 0.3017 (4) | 2.9 (2) |
| C27 | 0.500 (2) | 0.1764 (5) | 0.419 (1) | 2.7 (7) |
| O27 | 0.495 (1) | 0.1880 (4) | 0.4951 (8) | 4.9 (6) |
| | | Complex 3 | | |
| Au | 0.13891 (2) | 0.14079 (4) | 0.2500 (0) | 2.58 (1) |
| Co1 | 0.17926 (9) | 0.3203 (2) | 0.3164 (2) | 2.79 (6) |
| Co2 | 0.11549 (9) | 0.3235 (1) | 0.1792 (2) | 2.61 (6) |
| Co3 | 0.06527 (9) | 0.2812 (1) | 0.3223 (1) | 2.70 (6) |
| Fe | 0.0981 (1) | 0.4639 (2) | 0.2988 (2) | 3.60 (7) |
| P1 | 0.1442 (2) | −0.0290 (2) | 0.2656 (3) | 2.6 (1) |
| P2 | 0.1270 (2) | 0.2269 (3) | 0.0677 (3) | 3.2 (2) |
| P3 | 0.2612 (2) | 0.2302 (4) | 0.3427 (4) | 4.2 (2) |
| | | Complex 4 | | |
| Au | 0.29182 (7) | 0.0035 (2) | 0.11075 (6) | 2.95 (1) |
| Co1 | 0.1804 (2) | −0.0666 (5) | 0.1182 (2) | 2.84 (2) |
| Co2 | 0.2559 (2) | −0.1876 (5) | 0.0920 (2) | 2.79 (3) |
| Co3 | 0.2637 (2) | −0.1289 (5) | 0.1763 (2) | 2.95 (5) |
| Fe | 0.1812 (3) | −0.2560 (5) | 0.1460 (2) | 3.87 (11) |
| P1 | 0.3696 (5) | 0.1047 (9) | 0.0965 (4) | 3.0 (3) |
| P2 | 0.1575 (5) | 0.0927 (10) | 0.0963 (5) | 3.5 (9) |

[a] Remaining positional and thermal parameters are included in the supplementary material. [b] $B$ values for anisotropically refined atoms are given in the form of the isotropic equivalent thermal parameter defined as $^4/_3[a^2\beta_{11} + b^2\beta_{22} + c^2\beta_{33} + ab(\cos\gamma)\beta_{12} + ac(\cos\beta)\beta_{13} + bc(\cos\alpha)\beta_{23}]$.

Detailed distance and angle listings and tables of the remaining positional and thermal parameters have been included as suplementary material.

The raw data were processed on the PDP 11/45 computer by using the programs in the structure determination package SDP. Only data with $I \geq 3\sigma(I)$ were considered observed for least-squares refinement. For structures containing gold, the positions of the gold atoms were calculated from a Patterson map. For the other two structures, the positions of the iron and cobalt atoms were found via the direct-methods package MULTAN. The positions of the remaining non-hydrogen atoms were found by subsequent least-squares refinements and different Fourier syntheses. The positions of the hydrogen atoms were assigned by using standard C–H bond parameters. The hydrogen atoms then were added as fixed contributions to the structure with an isotropic temperature factor of 5.0 Å³.

**$[Et_4N][FeCo_3(CO)_{11}PPh_3]$ ([Et₄N][1]).** Crystals were grown by slow cooling of a saturated diethyl ether solution of $[Et_4N]$[1]. An irregularly shaped crystal of dimensions 1.33 × 0.45 × 0.10 mm was used. The space group was found to be $P\bar{1}$ (No. 2). Data were collected with a maximum scan time of 60 s. Because of the irregular shape of this crystal, an absorption correction could not be applied. The final unweighted and weighted residual values were 0.0459 and 0.0586, respectively.

**$[Co(CO)\{P(OMe)_3\}_4][FeCo_3(CO)_{11}P(OMe)_3]$ ([Co(CO)L₄][2]).** Crystals suitable for X-ray study were shown by slow cooling of a saturated diethyl ether solution of the purple oil from the synthesis reported above. A crystal with dimensions 0.075 × 0.175 × 0.450 mm was used. The space group was found to be $P2_1/c$ (No. 14) from the systematic absences of $k = 2n + 1$ for $0k0$ and $l = 2n + 1$ for $h0l$. An absorption correction was applied to the data. The final unweighted and weighted residual values were 0.048 and 0.069, respectively.

**$[Ph_3PAuFeCo_3(CO)_{10}\{P(OMe)_3\}_2]$ (3).** Crystals suitable for X-ray study were grown by slow cooling of a saturated toluene–hexane solution of **3**. A crystal of dimensions 0.20 × 0.40 × 0.30 mm was used. The space group was found to be $Pna2_1$ (No. 33) from the systematic absences of $h = 2n + 1$ for $h0l$ and $k + l = 2n + 1$ for $0kl$. While the structure was being solved, it was found that one of the carbon atoms of one of the trimethyl phosphites would not refine to one position but rather refined to two positions with partial occupancies of 0.5 each. They are referred to as C16A and C16B. An absorption correction was applied to the data. The final unweighted and weighted residual values were 0.041 and 0.049, respectively.

**$[Ph_3AuFeCo_3(CO)_{11}PMe_2Ph]$ (4).** Crystal were grown either one of two ways, each way producing crystals with different unit cells and space groups. When the crystals were grown by slow diffusion of hexane into a saturated toluene solution of **4**, crystals in space group $P2_1/c$ (No. 14) are obtained. When the crystals were grown by slow diffusion of pentane into a saturated toluene solution of **4**, crystals in the space group $C2/c$ (No. 15) are obtained. These crystals apparently decomposed due to loss of solvent since they deteriorated under nitrogen if not encased in mineral oil. Problems occurred with both sets of crystals, and neither set of crystals gave high-quality X-ray data. The $C2/c$ variant gave a data set that at least allowed us to solve the structure. The crystal was encased in mineral oil with a small amount of toluene added. The completed crystal structure showed a toluene of crystallization located along one of the 2-fold crystallographic axes (at $x = 0.0$ and $z = 0.25$). It was added to the structure as a fixed contribution (similar to the hydrogen atoms). The methyl of the toluene was not found in any different Fourier synthesis was and assumed to be disordered. An absorption correction was applied to the data. The final weighted and unweighted residual values were 0.089 and 0.101, respectively.

## Results and Discussion

The structures of the tetranuclear dodecacarbonyl cluster compounds and their phosphine-substituted derivatives have been the subject of many important and significant studies in inorganic chemistry. The final elucidation of the structure of the most important member of the series, $[Co_4(CO)_{12}]$, was a long and difficult quest. Early studies by Wei and Dahl[8] revealed the basic

**Table III.** Average Bond Distances (Å)[a]

| | 5⁻ | 1⁻ | 2⁻ | 6 | 3 | 4 |
|---|---|---|---|---|---|---|
| Au–Co | | | | 2.715 (6) | 2.72 (3) | 2.71 (3) |
| Fe–Co | 2.524 (7) | 2.55 (2) | 2.533 (6) | 2.59 (4) | 2.60 (3) | 2.60 (3) |
| Co–Co | 2.481 (8) | 2.51 (2) | 2.47 (2) | 2.52 (2) | 2.50 (2) | 2.53 (2) |
| Au–P | | | | 2.281 (4) | 2.283 (3) | 2.292 (7) |
| Co–P | | 2.246 (1) | 2.150 (4) | | 2.16 (2) | 2.247 (9) |
| $Co–C_t$ | 1.77 (4) | 1.77 (1) | 1.78 (4) | 1.75 (6) | 1.74 (5) | 1.72 (9) |
| $Co–C_b$ | 1.95 (3) | 1.93 (3) | 1.90 (7) | 1.94 (7) | 1.92 (5) | 1.88 (10) |
| $Fe–C_t$ | 1.77 (3) | 1.78 (2) | 1.83 (7) | 1.8 (2) | 1.71 (9) | 1.77 (7) |
| $(C–O)_t$ | 1.15 (3) | 1.14 (1) | 1.12 (4) | 1.20 (9) | 1.20 (6) | 1.15 (6) |
| $(C–O)_b$ | 1.14 (2) | 1.16 (1) | 1.20 (4) | 1.24 (2) | 1.17 (1) | 1.22 (6) |
| P–C | | 1.834 (4) | | 1.842 (4) | 1.82 (3) | 1.84 (6) |
| C–C | | 1.378 (10) | | 1.4 (1) | 1.36 (1) | 1.37 (8) |
| P–O | | | 1.56 (2) | | 1.57 (3) | |
| O–C | | | 1.42 (3) | | 1.57 (3) | |

[a] The compound numbering scheme in this and other tables is as follows: **1⁻**, $[FeCo_3(CO)_{11}PPh_3]^-$; **2⁻**, $[FeCo_3(CO)_{11}P(OMe)_3]^-$; **3**, $[Ph_3PAuFeCo_3(CO)_{10}\{P(OMe)_3\}_2]$; **4**, $[Ph_3PAuFeCo_3(CO)_{11}PMe_2Ph]$; **5⁻**, $[FeCo_3(CO)_{12}]^-$; **6**, $[Ph_3PAuFeCo_3(CO)_{12}]$.

**Table IV.** Average Bond Angles (deg)

| | $5^-$ | $1^-$ | $2^-$ | 6 | 3 | 4 |
|---|---|---|---|---|---|---|
| Co–Au–Co | | | | 55.3 (4) | 54.8 (4) | 55.7 (5) |
| Fe–Co–Au | | | | 112.19 (14) | 114 (2) | 113 (2) |
| Au–Co–Co | | | | 62.23 | 62.4 (14) | 62.1 (9) |
| Co–Fe–Co | 58.9 (1) | 58.89 (5) | 58.3 (5) | 59.0 (2) | 57.3 (7) | 58.1 (1) |
| Co–Co–Co | 60.0 (3) | 60.0 (5) | 60.0 (8) | 60.0 (6) | 60.0 (6) | 60.0 (6) |
| Fe–Co–Co | 60.6 (2) | 60.6 (5) | 60.8 (3) | 60.5 (13) | 61.0 (11) | 61.0 (10) |
| Co–Au–P | | | | 148 (7) | 146 (14) | 146 (14) |
| Fe–Co–$C_e$ | 89 (2) | 83 (2) | 91 (1) | 78 (5) | 73.0 (14) | 74 (4) |
| Fe–Co–$C_a$ | 192 (2) | 172 (2) | 195 (2) | 172 (3) | 164.9 (2) | 168 (3) |
| Fe–Co–P | | 192.25 (12) | 194.5 (2) | | 169 (4) | 166.8 (3) |
| Au–Co–$C_e$ | | | | 168 (4) | 172.1 (14) | 172 (4) |
| Au–Co–$C_a$ | | | | 73 (3) | 78.7 (2) | 76 (2) |
| Au–Co–$C_b$ | | | | 84 (3) | 84 (3) | 81.8 (13) |
| Au–Co–P | | | | | 78 (4) | 81.7 (3) |
| Co–Co–$C_e$ | 134 (2) | 130 (5) | 136 (2) | 125 (5) | 123 (2) | 123 (3) |
| Co–Co–$C_a$ | 110 (2) | 123 (5) | 107 (2) | 125 (5) | 129.7 (2) | 127 (3) |
| Co–Co–$C_b$ | 110.2 (12) | 109 (2) | 109.5 (11) | 109 (3) | 109.3 (13) | 107 (3) |
| Co–Co–$C_b$ | 50.2 (9) | 49.5 (9) | 50 (2) | 49 (2) | 49 (2) | 48 (3) |
| Co–Co–P | | 109.7 (9) | 107.4 (10) | | 128 (3) | 130 (2) |
| Co–Fe–$C_t$ | 155 (2) | 155 (3) | 155 (3) | 156 (4) | 154 (3) | 155 (3) |
| Co–Fe–$C_t$ | 101 (2) | 100 (3) | 100 (3) | 100 (4) | 100 (3) | 100 (3) |
| $C_a$–Co–$C_e$ | 102.0 (10) | 95 (3) | 104.4 (7) | 96 (2) | 93.5 (7) | 95 (2) |
| $C_t$–Fe–$C_t$ | 96 (3) | 97 (3) | 95.7 (8) | 97 (7) | 97 (3) | 99 (3) |
| $C_t$–Co–$C_b$ | 96 (2) | 97 (3) | 97 (3) | 1 | 95 (5) | 94.8 (11) |
| $C_t$–Co–P | | 100.2 (1) | 102.8 (5) | | 98 (2) | 95 (5) |
| $C_b$–Co–$C_b$ | 159.6 (7) | 157 (3) | 156 (4) | 158 (4) | 159 (3) | 155 (5) |
| $C_b$–Co–P | | 96.6 (7) | 97.7 (6) | 81.8 (8) | 81.2 (10) | 84 (2) |
| Co–(C–O)$_t$ | 178 (2) | 175 (2) | 177 (2) | 163 (10) | 172 (5) | 168 (8) |
| Co–(C–O)$_b$ | 140 (3) | 140 (3) | 139 (4) | 134 (14) | 139 (4) | 137 (7) |
| Fe–(C–O)$_t$ | 177.1 (5) | 177 (6) | 177 (2) | 166 (9) | 172 (5) | 169 (9) |
| Co–P–O | | | 117 (4) | | 114 (5) | |
| Au–P–C | | | | 112 (3) | 114.5 (5) | 116 (3) |
| Co–P–C | | 116.3 (9) | | | | 112 (4) |

$C_{3v}$ structure with three of the 12 carbonyl ligands bridging the basal cobalt atoms. The analysis was complicated by a disorder within the unit cell. A subsequent in depth report by Wei[9] confirmed the structural details, but the disorder still prevented an accurate determination of bond distances and angles. Several years later, Cotton attempted to sort out the disorder and with better data did determine a still flawed but somewhat more precise geometry for the molecule.[10]

The corresponding Rh compound, $[Rh_4(CO)_{12}]$, presented a similar structural problem. Twinning prevented a precise structure determination for the molecular structure, which was found to have a similar $C_{3v}$ geometry.[11] In contrast, the Ir compound, $[Ir_4(CO)_{12}]$, has an ordered structure with only terminal carbonyls.[12] The structure has $C_3$ site symmetry, but deviates only slightly from the ideal $T_d$ symmetry.

Phosphine-substituted derivatives of all three metals are based on the $C_{3v}$ structure with bridging carbonyls. Initial phosphine substitution invariably takes place at one of the three basal metal sites.[12] In cobalt derivatives, the axial carbonyl site seems to be preferred. Darensbourg and Incorvia found axial substitution in the monosubstituted phosphine derivative, $[Co_4(CO)_{11}PPh_3]$, and in the disubstituted phosphite derivative, $[Co_4(CO)_{10}\{P(OMe)_3\}_2]$.[13] In contrast, the triphenylphosphine derivatives of $[Ir_4(CO)_{12}]$ show equatorial site occupation as well. In the disubstituted compound, $[Ir_4(CO)_{10}\{PPh_3\}_2]$, one phosphine occupies an axial position on one basal Ir and the second phosphine occupies an equatorial site on a second basal Ir. In the trisubstituted compound, $[Ir_4(CO)_9\{PPh_3\}_3]$, two phosphines are equatorial and only one is axial.[14]

Recently, we developed a force field procedure for simulating and evaluating the structures of metal carbonyl cluster compounds.[15] These calculations revealed that the $[M_4(CO)_{12}]$ molecules are relatively strain-free molecules when compared to certain other cluster compounds such as $[Fe_3(CO)_{12}]$.[16] This is a simple function of the change in coordination number from an average of four carbonyls per metal in $[Fe_3(CO)_{12}]$ to three carbonyls per metal in $[Co_4(CO)_{12}]$. The strain shows up directly in the metal–metal bond distances; ligand strain opens the Fe–Fe distances in $[Fe_3(CO)_{12}]$ to an average of 2.64 Å, while the unstrained Co–Co bonds in $[Co_4(CO)_{12}]$ average 2.49 Å. The correlation between ligand strain and metal–metal bond distances is a general one found for other metal carbonyl systems as well. The lack of strain in the $M_4(CO)_{12}$ molecule suggests that the steric constraints governing phosphorus ligand substitution may not be all that great.

The mixed-metal cluster anion $[FeCo_3(CO)_{12}]^-$ undergoes substitution reactions less readily than does the isostructural $[Co_4(CO)_{12}]$ molecule.[6] Under even more rigorous conditions, only monophosphine substitution takes place with the anion (with monodentate ligands), while under the same conditions, three or four phosphines can be substituted for carbonyls in the all cobalt compound. On the other hand, the molecular mixed-mixed hydride, $[HFeCo_3(CO)_{12}]$, is much more labile than the anion, although still less reactive than $[Co_4(CO)_{12}]$.[17] For example, a simple reflux in hexane, gives the trisubstituted trimethyl phosphite derivative.[18]

$$[FeCo_3(CO)_{12}]^- + \text{excess } P(OMe)_3 \xrightarrow[\text{acetone}]{\Delta} [FeCo_3(CO)_{11}P(OMe)_3]^- + CO \quad (1)$$

$$[HFeCo_3(CO)_{12}] + \text{excess } P(OMe)_3 \xrightarrow[\text{hexane}]{\Delta} [HFeCo_3(CO)_9\{P(OMe)_3\}_3] + 3CO \quad (2)$$

(8) Wei, C. H.; Dahl, L. F. *J. Am. Chem. Soc.* **1966**, *88*, 1821.
(9) Wei, C. H. *Inorg. Chem.* **1969**, *8*, 2384.
(10) Carre, F. H.; Cotton, F. A.; Frenz, B. A. *Inorg. Chem.* **1976**, *15*, 380.
(11) Wei, C. H.; Wilkes, G. R.; Dahl, L. F. *J. Am. Chem. Soc.* **1967**, *89*, 4792.
(12) Churchill, M. R.; Hutchinson, J. P. *Inorg. Chem.* **1978**, *17*, 3528.
(13) Darensbourg, D. J.; Incorvia, M. J. *Inorg. Chem.* **1980**, *19*, 1911.
(14) Albano, V.; Bellon, P. L.; Scatturini, V. *Chem. Commun.* **1967**, *730*.
(15) Lauher, J. W. *J. Am. Chem. Soc.* **1986**, *108*, 1521.
(16) Cotton, F. A.; Troup, J. M. *J. Am. Chem. Soc.* **1974**, *96*, 4155.
(17) Cooke, C. G.; Mays, M. J. *J. Chem. Soc., Dalton Trans.* **1975**, 455.
(18) Huie, B. T.; Knobler, C. B.; Kaesz, H. D. *J. Am. Chem. Soc.* **1978**, *100*, 3059. Teller, R. G.; Wilson, R. D.; McMullan, R. K.; Koetzle, T. F.; Bau, R. *Ibid.* **1978**, *100*, 3071.

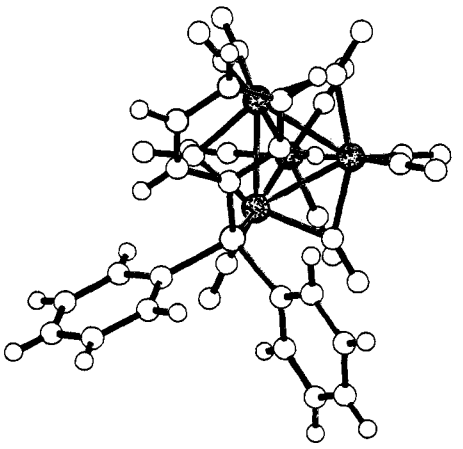

**Figure 1.** ROTOCHEM[7] drawing of $[FeCo_3(CO)_{11}PPh_3]^-$ anion of $[Et_4N][FeCo_3(CO)_{11}PPh_3]$ looking at the tricobalt face. Note that one of the phenyl rings almost entirely blocks the face.

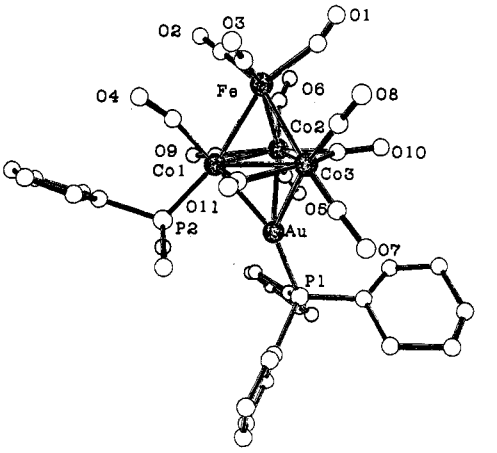


**Figure 2.** ROTOCHEM drawing of $[Ph_3PAuFeCo_3(CO)_{11}PMe_2Ph]$. Note the bend of the $Ph_3PAu$ moiety away from the phosphine.

This increase in lability of the carbonyls in $[HFeCo_3(CO)_{12}]$ when compared to that of the anionic $[FeCo_3(CO)_{12}]^-$ follows the experimental observation that anionic carbonyl complexes are more difficult to substitute than similar neutral complexes, for example, substitution of $M(CO)_6$ (M = Cr, Mo, W) vs $M(CO)_6^-$ (M = V, Nb, Ta).[19] It is also consistent with a dissociative CO-substitution mechanism. It would follow from these observations that the gold adduct compound, $[Ph_3PAuFeCo_3(CO)_{12}]$, being neutral, would also be quite labile to phosphine substitution showing behavior similar to that of the $[HFeCo_3(CO)_{12}]$ cluster. In addition, the open coordination site on the gold atom could potentially increase the lability of the cluster by providing a site for an associative ligand substitution.

When a phosphine is added to a solution of $[Ph_3PAuFeCo_3(CO)_{12}]$, an immediate reaction occurs where the phosphine does indeed appear to attack the gold atom. The result is a dissociation of the cluster. The end products are a $[Ph_3PAuPR_3]^+$ cation and a $[FeCo_3(CO)_{12}]^-$ anion. A similar reaction has been observed for $[Ph_3PAuRuCo_3(CO)_{12}]$ by Braunstein.[20]

$$[Ph_3PAuFeCo_3(CO)_{12}] + PPh_3 \rightarrow [Ph_3PAuPPh_3]^+ + [FeCo_3(CO)_{12}]^- \quad (3)$$

There is, of course, another potential route of obtaining phosphine- (or phosphite-) substituted derivatives of $[Ph_3PAuFeCo_3(CO)_{12}]$. This route consists of first carrying out a substitution of the anion, $[FeCo_3(CO)_{12}]^-$, with a phosphorus ligand and then allowing the substituted anion to react with $[Ph_3PAuNO_3]$ to give the substituted gold adduct compound.

$$[FeCo_3(CO)_{12}]^- + PR_3 \xrightarrow[\text{acetone}]{\Delta} [FeCo_3(CO)_{11}PR_3]^- + CO \quad (4a)$$

$$[FeCo_3(CO)_{11}PR_3]^- + [Ph_3PAuNO_3] \xrightarrow[CH_2Cl_2]{} [Ph_3PAuFeCo_3(CO)_{11}PR_3] + NO_3^- \quad (4b)$$

This reaction was first attempted with triphenylphosphine. The substituted anion, $[FeCo_3(CO)_{11}PPh_3]^-$, is a known anion that can be easily prepared.[6] The addition of an acid to a reddish purple solution of $[FeCo_3(CO)_{11}PPh_3]^-$ is accompanied by an immediate color change to the deep blue-purple color of the hydride.

A similar addition of $[Ph_3PAuNO_3]$ to a solution of $[FeCo_3(CO)_{11}PPh_3]^-$ gives no observed spectral changes, and indeed no reaction has been observed. Since $Ph_3PAuNO_3$ reacts readily with the all carbonyl compound, $[FeCo_3(CO)_{12}]^-$, this lack of reactivity with the triphenylphosphine-substituted compound would appear to be due to a steric problem associated with the axial coordination of the phosphine. In the molecular structure of the triphenylphosphine compound the tricobalt face of the anion is indeed blocked by one phenyl of the phosphine ligand (Figure 1).

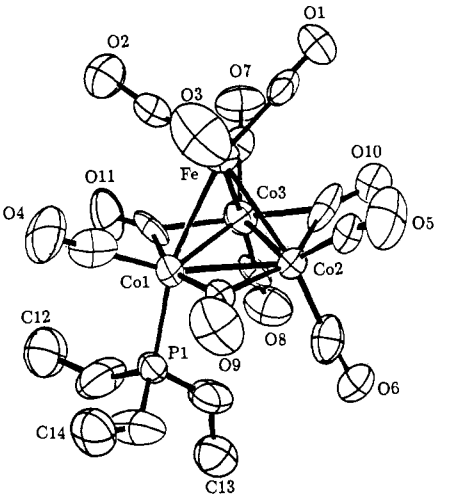


**Figure 3.** ORTEP drawing of the $[FeCo_3(CO)_{11}P(OMe)_3]^-$ anion of $[Co(CO)\{P(OMe)_3\}_4][FeCo_3(CO)_{11}P(OMe)_3]$.

To probe this steric effect further, the reaction was repeated using a smaller phosphine ligand, dimethylphenylphosphine. In this case, the reaction proceeds cleanly, giving a deep blue green solution of the compound $[Ph_3PAuFeCo_3(CO)_{11}(PMe_2Ph)]$. An examination of its molecular structure shows the lone phenyl ring of the dimethylphenylphosphine turned away from the gold atom, which is bonded to the tricobalt face, Figure 2. The triphenylphosphine coordination to the gold atom takes an off-axis geometry to further avoid close contacts with the dimethylphenylphosphine ligand.

As mentioned earlier, trimethyl phosphite will react with the cluster hydride, $[HFeCo_3(CO)_{12}]$, to give the trisubstituted product, $[HFeCo_3(CO)_9\{P(OMe)_3\}_3]$, but even with an excess of phosphite, the reaction of the $[FeCo_3(CO)_{12}]^-$ anion with trimethyl phosphite will give only the monosubstituted product, $[FeCo_3(CO)_{11}P(OMe)_3]^-$. The actual synthesis and isolation of the monosubstituted anion is difficult, because of the physical properties of the product. Crystalline samples are difficult to prepare, oils being obtained instead. In addition, a certain amount of decomposition to give oxidized metal cations always seems to take place. The only crystalline samples of $[FeCo_3(CO)_{11}P(OMe_3)]^-$ isolated were shown by X-ray crystallography to contain the unusual countercation $[Co(CO)\{P(OMe)_3\}_4]^+$. In all of our preparations, the exact nature of the countercation remained somewhat of a mystery.

An examination of the molecular structure of the trimethyl phosphite-substituted anion showed axial coordination of the

(19) Dobson, G. R.; Stolz, I. W.; Shelini, R. K. *Adv. Inorg. Chem. Radiochem.* **1966**, *8*, 1, Davison, A.; Ellis, J. E. *J. Organomet. Chem.* **1971**, *31*, 239.

(20) Braunstein, P.; Rose, J.; Dediere, A.; Dusausorg, Y.; Mangiot, J. P.; Tiripicchio, A.; Tiripicchio-Camellini, M. *J. Chem. Soc., Dalton Trans.* **1986**, 225.

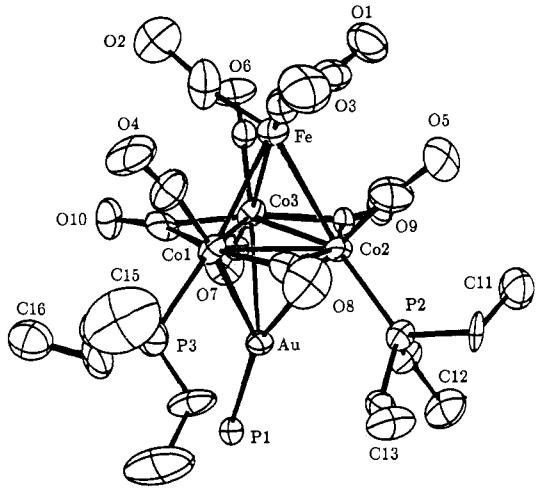


**Figure 4.** ORTEP drawing of $[Ph_3PAuFeCo_3(CO)_{10}\{P(OMe)_3\}_2]$. The phenyl rings are omitted for clarity.

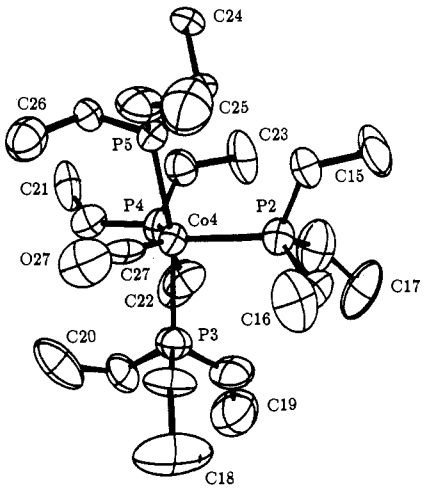


**Figure 5.** ORTEP drawing of the $[Co(CO)\{P(OMe)_3\}_4]^+$ cation of $[Co(CO)\{P(OMe)_3\}_4][FeCo_3(CO)_{11}P(OMe)_3]$. Note that the arrangement of the ligands about the central cobalt atom is intermediate between trigonal bipyramidal and square pyramidal.

phosphite, but no significant blocking of the tricobalt face (see Figure 3). In keeping with this observation, $[Ph_3PAuNO_3]$ readily reacts with solutions of $[FeCo_3(CO)_{11}P(OMe)_3]^-$ to give green-blue solutions of a gold adduct. Subsequent crystallization of this product followed by an X-ray structure determination revealed a most surprising result. The product consisted of the gold adduct of the disubstituted anion, $[Ph_3PAuFeCo_3(CO)_{10}\{P(OMe)_3\}_2]$, and not the expected monosubstituted product.

The source of the second phosphite is somewhat of a mystery, but there are several possibilities. There is no evidence of a disubstituted impurity in the preparation of the monosubstituted reactant, but a simple odor test revealed that excess trimethyl phosphite is difficult to remove from the oily product. The countercation is also a possible source since we have actually characterized a sample containing the $[Co(CO)\{P(OMe)_3\}_4]^+$ cation. Finally, during purification of the substituted gold derivative, nonsubstituted $[FeCo_3(CO)_{12}]^-$ was isolated. Since there was no evidence of this ion when the monosubstituted phosphite reactant was purified by column chromatography, we can assume that it is a side product of the gold reaction. Perhaps some exchange or disproportionation reaction has occurred.

Wherever the extra phosphite did come from, it seemed that all crystals grown from different batches from this reaction were of the disubstituted gold derivative. Infrared analyses of all the phosphite-substituted products appeared to be rather similar and were not of much help in sorting out the problem. Individual crystals suitable for X-ray analysis were readily grown from each reaction mixture, but no satisfactory analytically pure sample could be obtained. The results of carbon and hydrogen analyses tended to be inconsistent and suggestive of impure product mixtures, containing less than two trimethyl phosphites per cluster.

The molecular structure of $[Ph_3PAuFeCo_3(CO)_{10}\{P(OMe)_3\}_2]$ (see Figure 4) was thus an unexpected bonus to this study. As discussed below it also has a somewhat asymmetric gold coordination, but not quite as much as found in the $PMe_2Ph$ compound.

**Crystallographic Results.** The molecular structures of two monosubstituted $[FeCo_3(CO)_{12}]^-$ anions and two substituted $[Ph_3PAuFeCo_3(CO)_{12}]$ molecules have been determined. Crystallographic parameters for the four compounds are given in Table I. Positional and thermal parameters for the core atoms are listed in Table II. Average bond distances and angles are listed in Table III and IV. Detailed distance and angles lists and the positional and thermal parameters have been included as supplementary material.

**Identification of Fe Atom.** The location of the Fe atom within these clusters cannot be assigned on the basis of our crystallographic results, since the electron densities of Fe and Co are not sufficiently distinguishable. The Fe has been assumed to occupy the apical position, because of the apparent symmetry of the carbonyls within the molecules and the relative simplicity of the infrared spectra of the compounds. One can also make an analogy to the known structure of the substituted hydride derivative, $[HFeCo_3(CO)_9\{P(OMe)_3\}_3]$. The hydride structure was determined by neutron diffraction, thus establishing unequivocally the apical position for the iron atom in that compound. All of the analogous $RuCo_3$ compounds are known to have apical Ru atoms.

**Table V.** Geometry of $[CoCO\{P(OMe)_3\}_4]^+$: Trigonal Bipyramidal or Square Pyramidal?

| plane no. | atoms in plane | plane no. | atoms in plane |
|---|---|---|---|
| 1 | P2, P4, P5 | 4 | C27, P3, P4 |
| 2 | P2, P3, P4 | 5 | C27, P2, P3 |
| 3 | C27, P4, P5 | 6 | C27, P2, P5 |

| angle[a] | ideal trigonal bipyramidal[b] | $[CoCO\{P(OMe)_3\}_4]^+$ | ideal square pyramidal[b] |
|---|---|---|---|
| $\delta_{36}$ | 101.5 | 107.6 | 118.5 |
| $\delta_{16}$ | 101.5 | 108.0 | 118.5 |
| $\delta_{45}$ | 101.5 | 109.6 | 118.5 |
| $\delta_{25}$ | 101.5 | 110.6 | 118.5 |
| $\delta_{13}$ | 101.5 | 95.6 | 76.9 |
| $\delta_{24}$ | 101.5 | 87.4 | 76.9 |
| $\delta_{12}$ | 53.1 | 68.0 | 76.9 |
| $\delta_{34}$ | 53.1 | 53.7 | 76.9 |
| $\delta_{56}$ | 53.1 | 26.9 | 0.0 |

[a] $\delta_{ij}$ = dihedral angle (deg) between planes $i$ and $j$. [b] See ref 21.

**$[Co(CO)\{P(OMe)_3\}_4]^+$ Cation.** The complex anion $[FeCo_3(CO)_{11}P(OMe)_3]^-$ was prepared by refluxing a solution of the $[FeCo_3(CO)_{12}]^-$ anion with an excess of $P(OMe)_3$. The product crystallized with an unusual cation, $[Co(CO)\{P(OMe)_3\}_4]^+$, evidently a result of a breakup of the reaction cluster anion. The molecular structure of this five-coordinate cobalt(I) cation is worthy of separate comment.

The actual geometry of the $[Co(CO)\{P(OMe)_3\}_4]^+$ cation is intermediate between that of a trigonal bipyramid with P5 and P3 in the axial positions or a square pyramid with P4 in the axial position, Figure 5. Muetterties developed a useful method of geometric analysis for five-coordinate structures based upon the dihedral angles between the triangular faces defined by adjacent ligating atoms.[21] The results of such an analysis, Table V, for this cation reveals values essentially halfway between ideal trigonal-bipyramidal and square-pyramidal values. The Co–P bond distances are significantly different with the trigonal-bipyramidal equatorial bond distances of 2.173 (4) and 2.176 (4) Å longer than the axial distances of 2.158 (4) and 2.151 (4) Å. The shorter M–P axial bond distances and the location of the CO ligand, the better $\pi$ acceptor in an equatorial position, is consistent with the

(21) Muetterties, E. L.; Guggenberger, L. J. *J. Am. Chem. Soc.* **1974**, *96*, 1748.

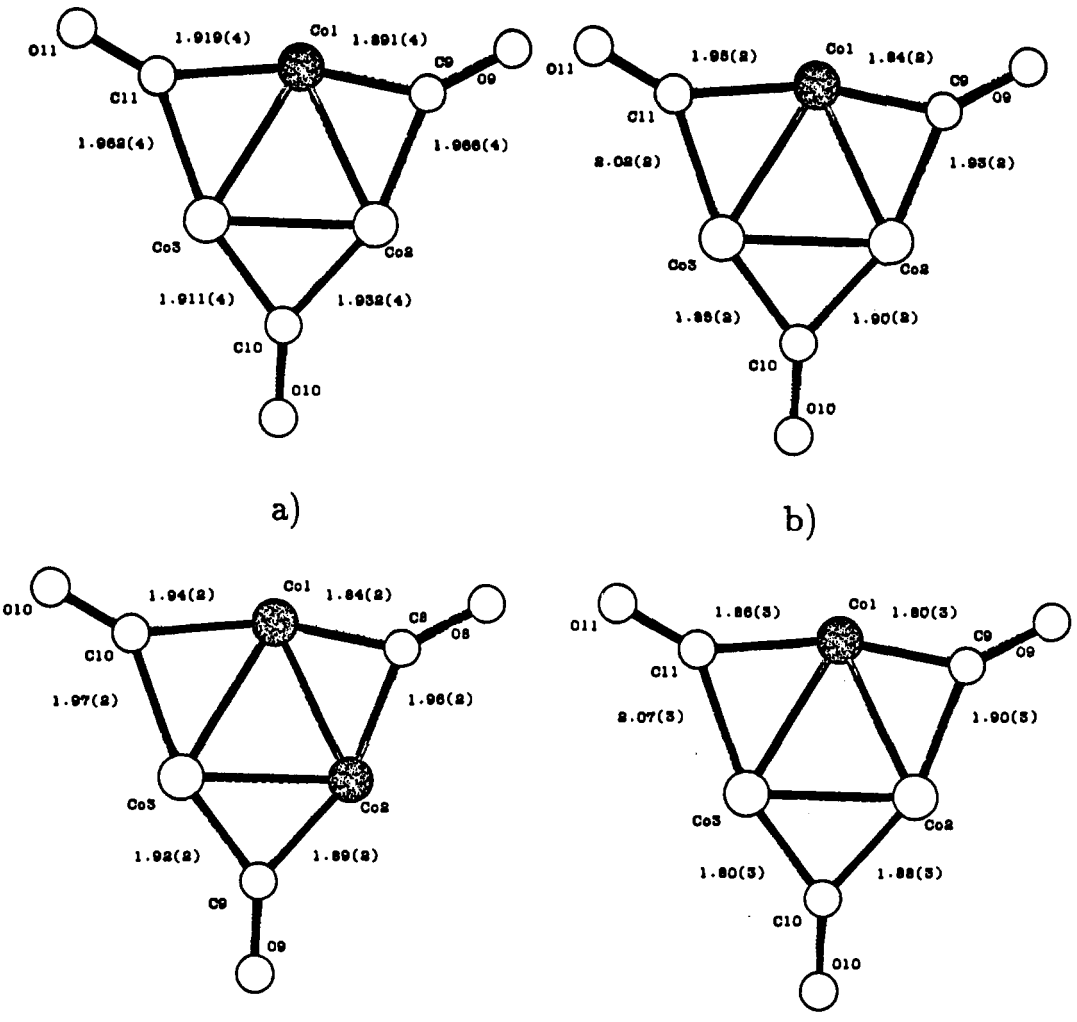


**Figure 6.** Cobalt–carbon bond distances of the bridging CO groups in (a) [$FeCo_3(CO)_{11}PPh_3$]$^-$, (b) [$FeCo_3(CO)_{11}P(OMe)_3$]$^-$, (c) [$Ph_3PAuFeCo_3(CO)_{10}\{P(OMe)_3\}_2$], and (d) [$Ph_3PAuFeCo_3(CO)_{11}PMe_2Ph$]. The substituted cobalt atoms are the speckled cobalts.

Hoffmann and Rossi predictions for a $d^8$ $ML_5$ trigonal bipyramid.[22]

**[$FeCo_3(CO)_{11}PPh_3$]$^-$ Anion.** The structure of the triphenylphosphine-substituted anion, shown in Figure 7, is similar to that of the analagous all-cobalt cluster, [$Co_4(CO)_{11}PPh_3$], reported by Darensbourg and Incorvia.[13] Both molecules have the triphenylphosphine in the axial position of a basal cobalt atom. The Co–P bond distance in the anion, 2.241 (1) Å, is similar to the 2.246 (1) Å distance in [$Co_4(CO)_{11}PPh_3$]. The angular disposition of the terminal ligands of the substituted cobalt atoms in the substituted anion is very similar to that found in the unsubstituted anion, [$FeCo_3(CO)_{12}$]$^-$, (Fe–Co–P angle of 192.25° vs a Fe–Co–$C_{ax}$ angle of 192 (2)°; P–Co–$C_{eq}$ angle of 100.2 (1)° vs a $C_{ax}$–Co–$C_{eq}$ angle of 102.0 (1)°).

Somewhat paradoxically the terminal carbonyl angular geometries about the two unsubstituted cobalt atoms are affected much more. The proximity of one of the phenyl rings of the phosphine ligand causes a 20° decrease in the axial carbonyl angles; the Fe–Co–$C_{ax}$ angle is 172 (2) vs 192.2 (1)° in the unsubstituted compound. The $C_{eq}$–Co–$C_{ax}$ angles are compressed by about 5° and the Fe–Co–$C_{eq}$ angles by about 10°. In the all-cobalt compound, [$Co_4(CO)_{11}PPh_3$], the phenyl ring closest to the cluster core has a somewhat different orientation and the corresponding angular distortions are only about half as large.

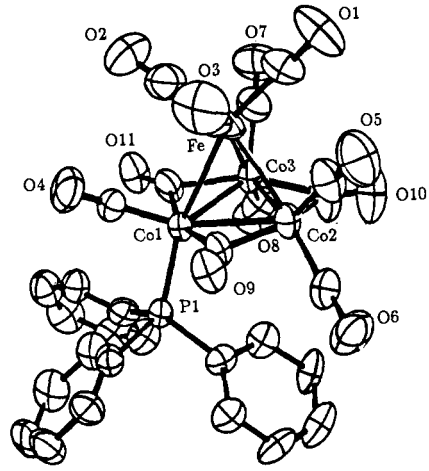


**Figure 7.** ORTEP drawing of the [$FeCo_3(CO)_{11}PPh_3$]$^-$ anion of [$Et_4N$][$FeCo_3(CO)_{11}PPh_3$].

One of the major structural effects found in the [$Co_4(CO)_{11}PPh_3$] structure was an asymmetry of the bridging carbonyls. The bridging carbonyls on the basal cobalt atoms were found to be closer to the substituted cobalt atom when bridging a substituted cobalt atom and a nonsubstituted cobalt atom. In addition, the Co–C–O angle was larger on the substituted side

(22) Rossi, A. R.; Hoffman, R. *Inorg. Chem.* **1975**, *14*, 365.

**Table VI.** Metal–Metal Bond Distances (in Å)

| | $5^-$ | $1^-$ | $2^-$ | 6 | 3 | 4 |
|---|---|---|---|---|---|---|
| Fe–Co1 | 2.525 (1) | 2.573 (1)[a] | 2.539 (1)[a] | 2.561 (3) | 2.610 (3)[a] | 2.628 (6)[a] |
| Fe–Co2 | 2.530 (2) | 2.531 (1) | 2.530 (3) | 2.600 (8) | 2.634 (3)[a] | 2.567 (6) |
| Fe–Co3 | 2.516 (2) | 2.552 (1) | 2.529 (3) | 2.515 (9) | 2.566 (2) | 2.616 (6) |
| Co1–Co2 | 2.488 (2) | 2.491 (1) | 2.467 (3) | 2.537 (8) | 2.492 (3) | 2.519 (5) |
| Co1–Co3 | 2.483 (2) | 2.505 (1) | 2.490 (3) | 2.506 (8) | 2.515 (3) | 2.547 (6) |
| Co2–Co3 | 2.472 (2) | 2.517 (1) | 2.450 (3) | 2.519 (3) | 2.488 (3) | 2.522 (5) |
| Au–Co1 | | | | 2.709 (2) | 2.742 (2)[a] | 2.739 (4)[a] |
| Au–Co2 | | | | 2.720 (5) | 2.713 (2)[a] | 2.697 (4) |
| Au–Co3 | | | | 2.716 (7) | 2.690 (2) | 2.686 (4) |

[a] These distances involve either one or two substituted cobalt atoms.

of the bridge. This asymmetry is found in the anion $[FeCo_3(CO)_{11}PPh_3]^-$ as well, as shown in Figure 6.

**$[FeCo_3(CO)_{11}P(OMe)_3]^-$ Anion.** The structure of this ion, shown in Figure 3, is much more like that of the all-carbonyl parent anion, $[FeCo_3(CO)_{12}]^-$, than is the triphenylphosphine-substituted anion discussed above. The smaller size of the trimethyl phosphite evidently does require the angular compression of the carbonyls found in the triphenylphosphine case. The asymmetry of the bridging carbonyls still exits, although the larger errors in this structure make it a bit less clear (see Figure 6).

**$[Ph_3PAuFeCo_3(CO)_{11}PMe_2Ph]$.** This compound can be considered as a derivative of the all-carbonyl compound, $[Ph_3PAuFeCo_3(CO)_{12}]$. That compound has a nearly ideal trigonal-bipyramidal cluster core with a pseudo-3-fold axis passing through the iron, gold, and phosphorus atoms.[5] In the $PhMe_2Ph$ compound, significant distortions from the ideal geometry are observed. The Au–Co bond distances are not equal, with a 2.739 (4) Å bond distance to the substituted cobalt atom, Co1, but shorter, 2.697 (4) and 2.686 (4) Å bond distances to the unsubstituted cobalt atoms. Interestingly the average Au–Co bond distance is nearly identical with the 2.715 (6) Å value found in the symmetrical, unsubstituted parent compound. The asymmetry of the $Ph_3PAu$ unit is shown more clearly by the Co–Au–P bond angle values of 162.6, 137.7 (2), and 138.1 (2)°. The larger angle again involves the substituted cobalt center. The dimethylphenylphosphine ligand is oriented such that the phenyl group is turned away from the gold atom. There are no close nonbonded contacts with the $PhMe_2Ph$ ligand.

All of the ligands of the original tetrahedral cluster are pushed up by the gold atom. The axial ligands on the basal cobalt atoms spread out, allowing the gold atom to bond to the cluster. In the anion, $[FeCo_3(CO)_{12}]^-$, the three axial carbonyls point inward toward the face with average Fe–Co–$C_{ax}$ angles of 192 (2)°. In the simple gold phosphine adduct, $[Ph_3PAuFeCo_3(CO)_{12}]$, these carbonyls are pushed out by 20° decreasing the Fe–Co–$C_{ax}$ angle to 172°. In the more crowded dimethylphenylphosphine complex, the axial ligands are pushed only slightly more with Fe–Co–$C_{ax}$ angles averaging 168 (3)° and an Fe–Co–P angle of 166.8°.

The equatorial carbonyl ligands on the basal cobalt atoms also move up such that the Fe–Co–$C_{eq}$ angles average 71°, bringing them into nearly semibridging positons. Although the angle errors are large, the equatorial carbonyl of Co2 is nonlinear with a 158 (3)° bond angle and a close (2.59 (3) Å) contact with the iron atom. The equatorial carbonyl on the substituted cobalt atom, Co1, is also bent with a 168 (3)° angle and a 2.69 (3) Å C···Fe contact, while the remaining equatorial carbonyl on Co3 is essentially linear with a longer (2.82 (3) Å) C···Fe contact.

**$[Ph_3PAuFeCo_3(CO)_{10}\{P(OMe)_3\}_2]$.** A single trimethyl phosphite ligand was found to cause only minor perturbations of the $[FeCo_3(CO)_{12}]^-$ anion structure; however, two such ligands cause structural distortions in the $[Ph_3PAuFeCo_3(CO)_{10}\{P(OMe)_3\}_2]$ molecule similar to the distortions resulting from a single $PMe_2Ph$ ligand in the $[Ph_3PAuFeCo_3(CO)_{11}PMe_2Ph]$ cluster. The gold atom in the $P(OMe)_3$ derivative has a similar asymmetry with Co–Au bond distances of 2.742 (2), 2.713 (2), and 2.690 (2) Å and corresponding Co–Au–P bond angles of 144.6 (1), 160.7 (1), and 132.8 (1)°.

The equatorial carbonyls of the basal carbonyl atoms are not pushed up quite as much in the $PMe_2Ph$ compound. The equatorial carbonyl on the unsubstituted cobalt atom, Co3, shows the greated distortion, with an Fe–Co–$C_{eq}$ angle of 71.6 (2)° and 166 (2)° bend of the Fe–C–O bond.

The axial phosphite ligands are pushed outward with Fe–Co–P angles of 166.0 (1) and 171.3 (2)°, while the axial carbonyl on Co3 is pushed out even more to an Fe–Co–$C_{ax}$ angle of 164.9 (2)°. The gold atom makes nonbonded contacts of 3.001 (4) and 3.217 (4) Å to the phosphorus atoms of the phosphite ligands and a 3.08 (1) Å contact with the nearest phosphite oxygen, O14. These distances are somewhat less than the sum of the respective van der Waals radii and may represent a slight attraction. The nonbonded contacts in the dimethylphenylphosphine structure are not so close.

**Metal–Metal Bond Distances.** Metal–metal bond distances for the parent all-carbonyl compounds and the four phosphorus-ligand-substituted compounds are listed in Table VI. Overall there is relatively little variation in the numbers, but a close examination reveals significant trends.

Phosphorus substitution results in slightly longer Fe–Co bond distances to the substituted cobalt atom. The differences are small, but they are found without exception in all four of the compounds studied. This same trend in the Fe–Co bond distances can also be found in the hydride compounds $[HFeCo_3(CO)_{10}\{PPh_3\}_2]$[23] and $[HFeCo_3(CO)_9\{PMe_2Ph\}_3]$.[24] Additionally, in the all-cobalt compounds studied by Darensbourg and Incorvia,[5] similar differences are found with slightly longer bond distances between the apical cobalt and the substituted basal cobalt atom. This small increase in metal–metal bond distance is consistent with an increase in electron density on the substituted cobalt, but is also consistent with a steric argument, since each of the phosphorus ligands caused increased steric congestion about the substituted metal center. In the unsubstituted anion, $[FeCo_3(CO)_{12}]^-$, there is very little variatioon in the Fe–Co bond distances. However, in the gold compound, $[Ph_3PAuFeCo_3(CO)_{12}]$, there are significant variations in the Fe–Co bond distances even though there is no substitution. However, the average Fe–Co bond distance in the gold compound is less than the average Fe–Co bond distances in the substituted gold compounds.

The addition of a gold atom to the tricobalt face also seems to cause an increase in the Fe–Co bond distances. The effect is small, less than 0.1 Å, but appears consistently in all the compounds studied. This effect is nonexistent or at least even smaller in the hydride compounds. This suggests that it may be primarily a steric effect associated with the larger gold atom and not an "electronic" effect.

The bridged cobalt–cobalt bond distances are remarkably constant in all of the compounds and are consistently shorter than the nonbridged Fe–Co bonds. The asymmetry in the bridging carbonyls is not accompanied by a change in metal–metal bond lengths.

## Conclusions

When we first considered synthesizing phosphorus-ligand-substituted derivatives of $[Ph_3PAuFeCo_3(CO)_{12}]$, we envisioned possible structural changes in which steric hindrance from a phosphorus ligand would cause the triply bridging gold atom to

(23) Iiskola, E.; Pakkanen, T. *Acta Chem. Scand., Ser. A* **1984**, *A38*, 731.
(24) Bartl, K.; Boese, R.; Schmid, G. *J. Organomet. Chem.* **1981**, *206*, 331.

move away from the tricobalt face onto possibly another face of the cluster or to an edge-bridging position. However, our results show that the addition of $[Ph_3PAu]^+$ to derivatives of $[FeCo_3(CO)_{12}]^-$ is apparently very site specific. When the approach to the tricobalt face is blocked by a bulky ligand, the $[Ph_3PAu]^+$ cation will not react with the substituted anion. This may very well be a kinetic problem reflective of the centering of the electron density of the anion on the blocked tricobalt face.

We had also wanted to see if $[Ph_3PAuFeCo_3(CO)_{12}]$ was as labile to phosphine substitution as is the hydride compound $[HFeCo_3(CO)_{12}]$. Unfortunately, due to the electrophilic nature of the gold atom in the cluster, no conclusions can be drawn about the lability of the carbonyl ligands to phosphine substitution in the cluster since the phosphine first attacks at the gold atom rather than substitutes for a carbonyl. The isolation of the disubstituted compound, $[Ph_3PAuFeCo_3(CO)_{10}\{P(OMe)_3\}_2]$, seems to suggest a labilization of the carbon monoxide ligands toward phosphorus-ligand substitution. Perhaps $^{13}CO$ exchange studies would give a better indication of the lability of the carbonyl ligands in this cluster since a cationic gold carbonyl complex would not be particularly stable.

Finally, when a phosphorus ligand substitutes for a carbonyl ligand in the $[M_4(CO)_{12}]$ cluster family, or a metal fragment is added to an open face, the other carbonyl ligands are able to move away in order to relieve the steric congestion. This is in agreement with our observations from force field calculations that the $[M_4(CO)_{12}]$ family of clusters is relatively strain free.

**Acknowledgment.** This work is supported by the National Science Foundation under Grant CHE8216662. We thank Dr. S. Sherlock and the other members of our research group for their assistance.

**Registry No.** $[Et_4N][1]$, 110637-27-9; $[Co(CO)L_4][2]$, 110660-49-6; 3, 110661-32-0; $4\cdot C_7H_8$, 110613-97-3; $[Et_4N][FeCo_3(CO)_{12}]$, 53509-36-7; $[FeCo_3(CO)_{11}P(OMe)_3]^-$, 110613-95-1; $Ph_3PAuNO_3$, 14897-32-6; Co, 7440-48-4; Fe, 7439-89-6; Au, 7440-57-5.

**Supplementary Material Available:** For each of the four structures, listings of additional atomic coordinates and isotropic thermal parameters, anisotropic thermal parameters, and complete bond distances and angles (33 pages); listings of observed and calculated structure factors for the four structures (49 pages). Ordering information is given on any current masthead page.

Contribution from the Institute of Catalysis, Novosibirsk 630090, USSR

# Formation, Structure, and Reactivity of Palladium Superoxo Complexes

Eugeni P. Talsi, Vera P. Babenko, Alexandr A. Shubin, Victor D. Chinakov, Vyatcheslav M. Nekipelov, and Kirill I. Zamaraev*

*Received September 9, 1986*

Formation of palladium superoxo complexes in the reactions of palladium(II) acetate, propionate, trifluoroacetate, and bis(acetylacetonate) and palladium(0) tetrakis(triphenylphosphine) with hydrogen peroxide and potassium superoxide has been detected in solution by EPR. According to EPR parameters the superoxo complexes observed fall into two main types. The $g$ factor of type I complexes is closer to an axial symmetrical one than that of type II complexes. For type I complexes, $g_1 = 2.08-2.1$, $g_2 = 2.01$, and $g_3 = 2.001-2.002$, and for type II complexes, $g_1 = 2.075-2.085$, $g_2 = 2.027-2.04$, and $g_3 = 2.006-2.01$. The EPR spectrum of type I complexes resulting from the interaction of $H_2O_2$ with $Pd(OAc)_2$ in $CHCl_3$ has a hyperfine structure indicating coupling to one Pd nucleus: $A_1^{Pd} = 6.7$ G, $A_2^{Pd} = 3.0$ G, and $A_3^{Pd} = 4.5$ G. Type I superoxo complexes appear to be characteristic of trimeric Pd species, formed by palladium(II) acetate and palladium(II) propionate in poorly coordinating solvents (chloroform and benzene), while type II superoxo complexes are characteristic of monomeric Pd species, formed by palladium(II) acetate and palladium(II) propionate in well-coordinating solvents (acetonitrile, dimethyl sulfoxide) and by palladium(II) trifluoroacetate, palladium(II) acetylacetonate, and palladium(0) tetrakis(triphenylphosphine) in poorly coordinating solvents. When prepared via interaction with $KO_2$ in the presence of 18-crown-6 ether, the type I superoxo complex initially formed in palladium(II) acetate and palladium(II) propionate systems rapidly transforms to the more stable type II complex, presumably due to the destruction of the trimeric Pd species by the 18-crown-6 ether. Type I superoxo complexes are more reactive than those of type II. Type I complexes formed by palladium(II) acetate and palladium(II) propionate easily oxidize simple olefins and CO, while type II complexes are inert with respect to these compounds. The type I superoxo complex of palladium(II) acetate oxidizes ethylene to ethylene oxide, $1 \pm 0.1$ mol of ethylene oxide being formed per $1 \pm 0.3$ mol of the superoxo complex decomposed. No other products have been detected with NMR for this reaction. The same superoxo complex oxidizes propylene to propylene oxide and acetone in a 1:2 ratio, again no other products being detected with NMR. The reaction rates demonstrate the first-order dependences on concentration of both the superoxo complexes and the olefins. The pseudo-first-order rate constants, determined for reactions of palladium(II) acetate type I complex with various alkenes at 300 K in $CHCl_3$ with a large excess of the alkenes (0.3 M) over the superoxo complex (0.005 M), are as follows: $10^3k = 2.3$ s$^{-1}$ ($CH_2$=$CH_2$); 5.1 s$^{-1}$ (MeCH=$CH_2$); 5.1 s$^{-1}$ ($Me_2C$=$CH_2$); 1.2 s$^{-1}$ ($Me_2C$=$CMe_2$). For the oxidation of CO by the same complex, the pseudo-first-order rate constants determined with a large excess of CO (concentration about 0.01 M, determined by solubility of CO at 1 atm) over the superoxo complex ($3 \times 10^{-4}$ M) at various temperatures are as follows: $10^3k = 9$ s$^{-1}$ (266 K); 2 s$^{-1}$ (258 K); 1 s$^{-1}$ (238 K); 0.6 s$^{-1}$ (226 K). Quantum-chemical calculations suggest that for the monomeric $Pd(acac)O_2$ complex $\eta^2$-coordination of the $O_2^-$ ligand is energetically more advantageous than $\eta^1$-coordination. On this ground $\eta^2$-coordination can be assumed for relatively stable superoxo complexes of type II. $g$ values for more reactive palladium superoxo complexes of type I are similar to those of cobalt superoxo complexes, which, according to X-ray data, have $\eta^1$-coordination. On this basis $\eta^1$-coordination of the $O_2^-$ ligand can be assumed for palladium superoxo complexes of type I.

## Introduction

Superoxo complexes of transition metals are assumed to be key intermediates of many reactions of homogeneous catalytic oxidation.[1-4] The superoxo complexes of Ni(II), Zn(II), Co(II), Co(III), Fe(II), Fe(III), Ce(III), Cr(III), Ti(IV), Th(IV), Hf(IV), Zr(IV), Sn(IV), V(V), Nb(V), and Mo(VI) are known.[5-8] However, there are very few reliable quantitative data on their reactivity. The sole exception is oxidation of hindered phenols

(1) Mimoun, H.; Saussine, L.; Daire, E.; Postel, M.; Fischer, J.; Weiss, R. *J. Am. Chem. Soc.* **1983**, *105*, 3101.
(2) Nishinaga, A.; Tomita, H. *J. Mol. Catal.* **1980**, *7*, 179.
(3) Zombeck, A.; Drago, R. S.; Corden, B. B.; Gaul, J. H. *J. Am. Chem. Soc.* **1981**, *103*, 7580.
(4) Corden, B. B.; Drago, R. S.; Perito, R. P. *J. Am. Chem. Soc.* **1985**, *107*, 2903.
(5) Afanasiev, I. B. *Usp. Khim.* **1979**, *48*, 977.
(6) Sawyer, D. T.; Valentine, J. S. *Acc. Chem. Res.* **1981**, *14*, 393.
(7) Sawyer, D. T.; Gibian, M. J. *Tetrahedron* **1979**, *35*, 1471.
(8) Shuvalov, V. F.; Moravskii, A. P.; Lebedev, Ya. S. *Dokl. Akad. Nauk SSSR* **1977**, *235*, 877.

0020-1669/87/1326-3871$01.50/0 